PROCEEDINGS, 43rd Workshop on Geothermal Reservoir Engineering
Stanford University, Stanford, California, February 12-14, 2018
SGP-TR-213

The Impact of Pore-Scale Flow Regimes on Upscaling of Immiscible Two-Phase Flow in Geothermal Reservoirs

Picchi, D., and Battiato, I.,

Stanford University, Energy Resources Engineering

367 Panama St.

Stanford, CA, 94305, Country

e-mail: dpicchi@stanford.edu, ibattiat@stanford.edu

Keywords: upscaling, relative permeability, two-phase flow, porous medium, pore-scale flow regimes

ABSTRACT

Two-phase flow conditions are frequently encountered in geothermal reservoirs due to gradients in pressure and temperature. Since empirical or theoretical extensions of Darcy's law for immiscible two-phase flow have shown significant limitations in properly modelling flow at the continuum-scale, in this paper we start with the upscaled equations based on pore-scale flow regimes (i.e., the topology of flowing phases) recently developed by *Picchi and Battiato* (2018) to understand the impact that the topology of flowing phases may have on relative permeability estimates at geothermal reservoir conditions. We illustrate and quantify the effect of pore-scale flow regimes on relative permeability by focusing on core-annular and plug flow regimes in a capillary tube, as surrogates of the large- and small-ganglion dynamical regimes, respectively. We show that, for cases with lower viscosity ratios, typical of geothermal systems, differences in the relative permeability between plug and core-annular flows is considerable in the whole range of saturation and reaches peaks larger than 100% with respect the relative permeability computed for core-annular flow.

1. INTRODUCTION

Geothermal reservoirs are characterized by a continuous migration of hot water from a high-temperature heat source to the (cooler) earth surface. Due to significant variations in temperature and pressure, water may experience a phase-change yielding to two-phase flow conditions (water and steam), while gradients in phase density lead to buoyancy effects all over the reservoir. At the pore scale, the flow is dominated by surface tension forces and wall wetting properties and it is also strongly affected by the pore geometry. In fact, these types of systems are usually characterized by a small Eotvos number ($Eo = \Delta\rho g L^2/\sigma \ll 1$), and therefore, the flow characteristics are similar to microgravity systems, see *Brauner* (1990).

The most common approach to modelling immiscible two-phase flow in a porous medium is to consider an extension of Darcy's law for the multiphase flow scenario by introducing the concept of relative permeability at the continuum scale, see *Bear* (1972). Up to now, many upscaling approaches have been adopted, such as homogenization via multi-scale expansions (e.g., *Auriault* (1987), *Hornung* (1997), *Darly and Roose* (2015)), volume averaging methods (e.g., *Whitaker* (1986) and *Lasseux et al.* (2008)), thermodynamic-based approaches which explicitly accounts for the dynamics of the interfacial area (e.g., *Hassanizadeh and Gray* (1980, 1990), *Miller and Gray* (2005), *Niessner and Hassanizadeh*, (2008), *Gray et al.* (2015)), and the work by *Xu and Wang* (2014) who derived a viscous dissipation upscaled law. These models are widely used in applications, but they have shown limitations: while more classical models based on multiphase Darcy have limited predictive capabilities, more nuanced models which include additional physics, e.g. inertial effects and/or the dynamics of the interface between the wetting and non-wetting phases, may be difficult to parametrize.

This is expected since the phase topology of two-phase flow system in a porous medium can be rather complex and four possible flow regimes have been experimentally identified by *Avraam and Payatakes* (1995) in a glass-etched model pore network of the chamber-and-throat type: large-ganglion dynamics, small-ganglion dynamics, drop-traffic flow, and connected-pathway flow. The importance of accounting for the phase topology in the definition of the relative permeability coefficients has been recently stressed by a large number of researchers (*Datta et al.* (2014), *Ruckes et al.* (2015), *Armstrong et al.* (2016), *McClure et al.* (2016), *Armstrong et al.* (2017), *Reynolds et al.* (2017) and *Gao et al.* (2017)). Importantly it is speculated that the transition from connected pathways regime to an intermittent regime (e.g., ganglion-dynamics) can be identified as one of the causes of hysteric behavior. Following this direction, *Picchi and Battiato (2018)* developed a new set of macroscopic equations by upscaling the incompressible Navier-Stokes equation and formulating the closures for different flow regimes at the pore-scale. In particular, it is shown that the classical two-phase Darcy law is recovered only for a limited range of operative conditions and analytical expressions for relative permeability have been presented for the basic flow regimes in an idealized pore-scale geometry (a capillary tube).

In this work, we will discuss the ramifications of the work by *Picchi and Battiato (2018*) in the geothermal context referring to several practical (and representative) cases. We will specifically focus on the impact that core-annular and slug flow in a capillary tube have on estimates of relative permeabilities of the wetting and non-wetting phases. These two flow regimes correspond to the large- and small-ganglia dynamics, as described by *Avraam and Payatakes* (1995). Our main focus is to present trends in term of relative permeability curves for the typical conditions encountered in geothermal reservoirs. The paper is organized as follows. In Section 2 we report the upscaled two-phase flow equations for flow in a capillary for core annular (Section 2.1) and plug flow (Section 2.2) regimes, and report the corresponding relative permeabilities for the wetting and non-wetting phases. In Section 3 we quantify the impact of the topology of

the flowing phases (i.e. flow regimes) on estimating the relative permeabilities in water-steam systems at typical geothermal pressure-temperature conditions and demonstrate the importance of accounting for the appropriate topological features of the flowing phases. We conclude with Section 3, where we discuss future

2. UPSCALED EQUATIONS BASED ON TWO-PHASE FLOW REGIMES AT THE PORE-SCALE

Picchi and Battiato (2018) proposed a methodology which combines multiphase flow upscaled equations developed for different pore-scale flow regimes with a mapping of existence of flow regimes in terms of dimensionless parameters. Many works have pointed out that the limited predictive capability of upscaled two-phase flow in a porous medium is accentuated when the pore-scale flow regimes are not taken into account (Datta et al. (2014), Ruckes et al. (2015), Armstrong et al. (2016), McClure et al. (2016), Armstrong et al. (2017), Reynolds et al. (2017) and Gao et al. (2017)).

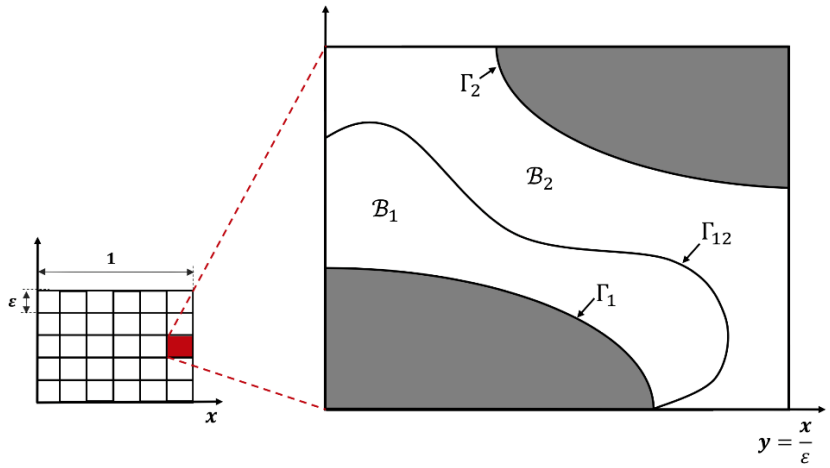

Figure 1: Schematic of the macroscopic domain and the unit cells defined in the homogenization process.

In this Section, we present, for completeness the sets of upscaled equations derived by Picchi and Battiato (2018) for the annular and plug-flow regimes in a capillary tube, as well as the main hypothesis underlying the upscaling method. The upscaled equations for averaged variables at the continuum scale (Darcy-scale) have been obtained by homogenization by means of multiple scales expansions: the main assumption behind such an analysis is that the separation of scales (between the continuum characteristic length L and the pore scale length l) holds. Referring to Fig. 1, we assume that the porous medium Ω can be represented as repetition of periodic unit cells Y occupied by two immiscible and incompressible fluids (region $\mathcal{B}_1$ and $\mathcal{B}_2$), while the scale parameter is defined as

$$\varepsilon = \frac{l}{L} \ll 1. \tag{1}$$

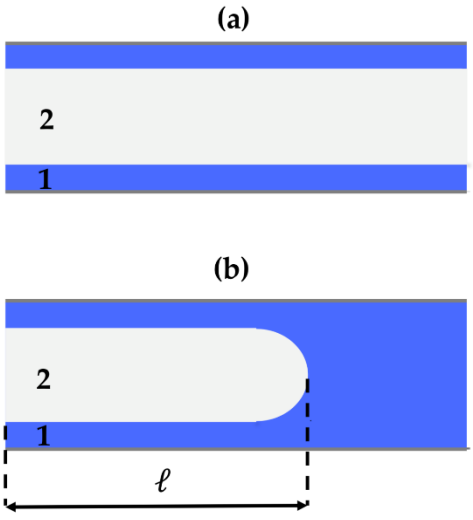

Figure 2: Sketch of flow regimes in a capillary tube: (a) core annular flow, (b) plug flow. Water (blue), steam (white).

The upscaled equations based on flow regimes have been presented referring to an idealized pore-scale geometry (a capillary tube). In particular, the basic flow regimes (core-annular flow and plug flow) in a capillary tube of constant diameter and in microgravity conditions, namely a low Eotvos number system, are considered, see Fig 2. An analogy with flow in a porous medium is rather straightforward: similarities between plug flow in a capillary tube and ganglia flow in a more complex porous medium are rather obvious, see for example the experimental results of *Ling et al.* (2017). In addition, modelling the two-phase flow in a capillary tube will provide the structure of the upscaled equation, which may be later generalized to a general porous medium. In the following, we report the sets of upscaled equations and corresponding effective parameters for annular and plug-flow regimes. All the details regarding the derivation can be found in *Picchi and Battiato* (2018).

2.1 Core-annular flow regime

A stable core-annular flow is obtained when the wetting phase flows in the annulus (in contact with the wall) while the non-wetting phase flows in the core, see Fig. 2(a). The upscaled equations for the case of laminar fully developed core-annular flow are

$$\varepsilon Re \mathrm{K}_1 \omega_1 \langle \overline{u_1} \rangle^2_{\mathcal{B}_1} = \left(-\nabla p_1 + \frac{\varepsilon^2 Re}{Fr^2} e_g \right) + 32 \left(M \frac{\langle \overline{u_2} \rangle_{\mathcal{B}_2} - 2\langle \overline{u_1} \rangle_{\mathcal{B}_1}}{S_1} - \frac{\langle \overline{u_1} \rangle_{\mathcal{B}_1}}{S_1^2} \right), \tag{2a}$$

$$\varepsilon RRe \mathrm{K}_2 \omega_2 \langle \overline{u_2} \rangle^2_{\mathcal{B}_2} = \left(-\nabla p_2 + \frac{\varepsilon^2 RRe}{Fr^2} e_g \right) + 32M \left(\frac{2\langle \overline{u_1} \rangle_{\mathcal{B}_1} - \langle \overline{u_2} \rangle_{\mathcal{B}_2}}{1 - S_1} \right), \tag{2b}$$

$$p_1 - p_2 = \frac{2\varepsilon}{Ca\sqrt{1-S_1}}, \tag{2c}$$

where the subscripts 1 and 2 refers to the annulus (wetting phase) and core (non-wetting phase), respectively. $Re = \rho_1 UL / \mu_1$, $R = \rho_2 / \rho_1$, $M = \mu_2 / \mu_1$, $Ca = \mu_1 U / \sigma$ are the Reynolds number, the density ratio, the viscosity ratio and the capillary number of the system. ∇p_i is the macroscopic pressure gradient, S_1 is the saturation, $\mathrm{K_i}$ is the relative permeability of phase *i* and is a function of the saturation only, ω_i is the shape factor which depends on the velocity profiles and is defined as

$$\omega_i = \frac{\langle \overline{u_i^3} \rangle_\Gamma}{\langle \overline{u_i} \rangle^3_{\mathcal{B}_i}}, \tag{3}$$

where Γ is the surface which bounds the volume $\mathcal{B}_i$ and $\langle \overline{u_i} \rangle_{\mathcal{B}_i}$ is the average velocity of the i-th phase over the volume occupied by the i-th phase.

Under the hypothesis that the inertia terms (l.h.s. of Eq. (2)) are negligible, the macroscopic pressure gradients for the two phases are equal to each other, and assuming microgravity conditions, we recover the Darcy's law as well as analytical expressions for the relative permeabilities, i.e.

$$\langle \overline{u_1} \rangle = -\frac{\phi K_{11}}{32} \nabla p_1 \quad \text{with} \quad K_{11} = S_1^2, \tag{4a}$$

$$\langle \overline{u_2} \rangle = -\frac{\phi K_{22}}{32M} \nabla p_2 \quad \text{with} \quad K_{22} = (2MS_1 - S_1 + 1)(1 - S_1), \tag{4b}$$

where ϕ is the porosity, $\langle \overline{u_i} \rangle$ is the average velocity of the i-th phase over the unit cell and is related to $\langle \overline{u_i} \rangle_{\mathcal{B}_i}$ through

$$\langle \overline{u_i} \rangle = \phi S_i \langle \overline{u_i} \rangle_{\mathcal{B}_i}, \tag{5}$$

The system is then closed with a conservation law for the saturation,

$$\phi \frac{\partial S_i}{\partial t} + \nabla \cdot \langle \overline{u_i} \rangle = 0 \ \text{ with } \quad i = 1,2 \ \text{ and } S_1 + S_2 = 1. \tag{6}$$

2.2 Plug flow regime

The plug flow regime (ganglia) in a capillary tube consists in a sequence of taps of a continuous phase (slug region of length $1 - \ell$) and elongated bubbles (or elongated drops in liquid-liquid systems), which are surrounded by a film of the continuous phase (plug region of length ℓ), see Fig. 2(b). In case the bubble/drop is sufficiently long, a region of a uniform film thickness is formed, and it can be modelled as a (local) region of fully developed core-annular flow, see *Picchi et al*. (2018). Assuming also that the unit cell Y contains an average (representative) plug unit cell, the upscaled equations for the plug flow regimes yield

$$\varepsilon Re \mathrm{K}_1 \omega_1 \langle \overline{u_1} \rangle^2_{\mathcal{B}_1} = \left(-\nabla p_1 + \frac{\varepsilon^2 Re}{Fr^2} e_g \right) + 32\ell \left(M \frac{\langle \overline{u_{2p}} \rangle_{\mathcal{B}_2} - 2\langle \overline{u_{1p}} \rangle_{\mathcal{B}_1}}{S_{1p}} - \frac{\langle \overline{u_{1p}} \rangle_{\mathcal{B}_1}}{S_{1p}^2} \right) + 32(1 - \ell) \langle \overline{u_{1s}} \rangle_{\mathcal{B}_1}, \tag{7a}$$

$$\varepsilon RRe \mathrm{K}_2 \omega_2 \langle \overline{u_2} \rangle^2_{\mathcal{B}_2} = \left(-\nabla p_2 + \frac{\varepsilon^2 RRe}{Fr^2} e_g \right) + 32M\ell \left(\frac{2\langle \overline{u_{1p}} \rangle_{\mathcal{B}_1} - \langle \overline{u_2 p} \rangle_{\mathcal{B}_2}}{1 - S_{1p}} \right), \tag{7b}$$

$$p_1 - p_2 \sim \frac{2\varepsilon\ell}{Ca\sqrt{1-S_1}}, \tag{7c}$$

where the subscripts p and s refer to the plug and slug regions, respectively. The system is closed by the conservation law for the saturation, Eq. (6), and the following relations for the saturation and the average velocities

$$S_1 = \ell S_{1p} + 1 - \ell, \tag{8a}$$

$$\langle \overline{u_1} \rangle_{\mathcal{B}_1} = \ell \langle \overline{u_{1p}} \rangle_{\mathcal{B}_1} + (1-\ell) \langle \overline{u_{1s}} \rangle_{\mathcal{B}_1}, \tag{8b}$$

$$\langle \overline{u_2} \rangle_{\mathcal{B}_1} = \ell \langle \overline{u_{2p}} \rangle_{\mathcal{B}_2}, \tag{8c}$$

$$\langle \overline{u_{1s}} \rangle_{\mathcal{B}_1} = S_{1p} \langle \overline{u_{1p}} \rangle_{\mathcal{B}_1} + \left(1 - S_{1p}\right) \langle \overline{u_{2p}} \rangle_{\mathcal{B}_2}, \tag{8d}$$

where S_{1p} is the saturation of the wetting phase within the plug region and it is related to the wetting phase thickness, namely the film thickness h in the elongated bubble (or drop) region, as

$$h = 1 - \sqrt{1 - S_{1p}} \ . \tag{9}$$

Note that h is the only closing parameter of the problem and can be determined, for example, by experiments or by theory-based correlations, such as the Bretherton law, *Bretherton* (1961), which expresses the film thickens as a function of the Capillary number, $h = h(Ca)$.

Under the assumption that the inertia terms (l.h.s. of Eq. (7)) are negligible, the macroscopic pressure gradient is the same for both phases, and assuming microgravity conditions, we recover the Darcy's law obtaining analytical expressions for the relative permeabilities:

$$\langle \overline{u_1} \rangle = -\frac{\phi K_{11}}{32} \nabla p_1 \quad \text{with} \quad K_{11} = \frac{\left[(1-M)S_{1p} - S_{1p}^3 + S_{1p}^2\right] S_1 + S_{1p}(S_{1p}-1)(S_{1p}^2 + M - 1)}{M\left[S_1\left(1 + S_{1p} - S_{1p}^2\right) + S_{1p}^3 - S_{1p}^2 - S_{1p} - 1\right]} S_1, \tag{10a}$$

$$\langle \overline{u_2} \rangle = -\frac{\phi K_{22}}{32M} \nabla p_2 \quad \text{with} \quad K_{22} = \frac{\left[S_{1p}^4 - S_{1p}^3 + (2M-1)S_{1p} + 1\right] - S_{1p}^5 + S_{1p}^4 + (1-2M)S_{1p} - 1}{(1-S_{1p})(S_{1p}^2 - S_{1p} - 1)S_1 + (S_{1p}-1)(S_{1p}^3 - S_{1p}^2 - S_{1p} - 1)} (S_1 - 1). \tag{10b}$$

Note that the relative permeabilities depend only on the unit cell saturation, S_1, the saturation in the plug region S_{1p}, and the viscosity ratio M. In the following section, we discuss the impact that the topology of the flowing phases has on relative permeability estimates for conditions typical of geothermal reservoirs.

3. DISCUSSION

In this section, we will discuss the ramifications of the upscaled equations described in Section 2 in the geothermal context. We will focus on scenarios where the inertia terms (l.h.s. of the upscaled equations) are negligible, see the applicability maps of *Picchi and Battiato (2018)* and on the range of dimensional parameters typical of geothermal reservoir. Since we are interested in two-phase flow conditions we will restrict our analysis to conditions where water is in a biphasic state, i.e. on water/steam systems. Table 1 reports the properties of water and saturated steam at typical temperatures of geothermal reservoir, see *Horne* (2016), and the corresponding viscosity and density ratio; note that water is the wetting phase while steam is the non-wetting phase. The liquid phase (water) is much more dense and viscous than steam, and therefore the systems of interest are characterized by small density and viscosity ratios, $R \ll 1$ and $M < 0$. In the following, we will show that different flow regimes at the pore-scale may significantly influence the relative permeability curves, focusing, in particular, on the core-annular and the plug flow regimes.

Table 1: Properties of water (w) and saturated steam (s) at temperatures typical of geothermal reservoirs.

T [°C]	p [bar]	ρ_w [kg/m³]	ρ_s [kg/m³]	μ_w [Pa s]	μ_s [Pa s]	R	M
260	46.9	783.6	23.7	0.0001	$1.79\ 10^{-5}$	0.03	0.18
120	2.0	943.1	1.1	0.0002	$1.30\ 10^{-5}$	0.01	0.07

Concerning the core-annular flow regime, the trends of K_{11} (i.e. relative permeability of the wetting phase) and K_{22} (i.e. relative permeability of the non-wetting phase) as function of the (water) saturation and the viscosity ratio are shown in Fig. 3. In particular, K_{11} is independent from the viscosity ratio, while $K_{22} \to (1 - S_1)^2$ as $M \to 0$. Note that the limit of very low viscosity ratio, $M \to 0$, is relevant in the geothermal context, see Table 1.

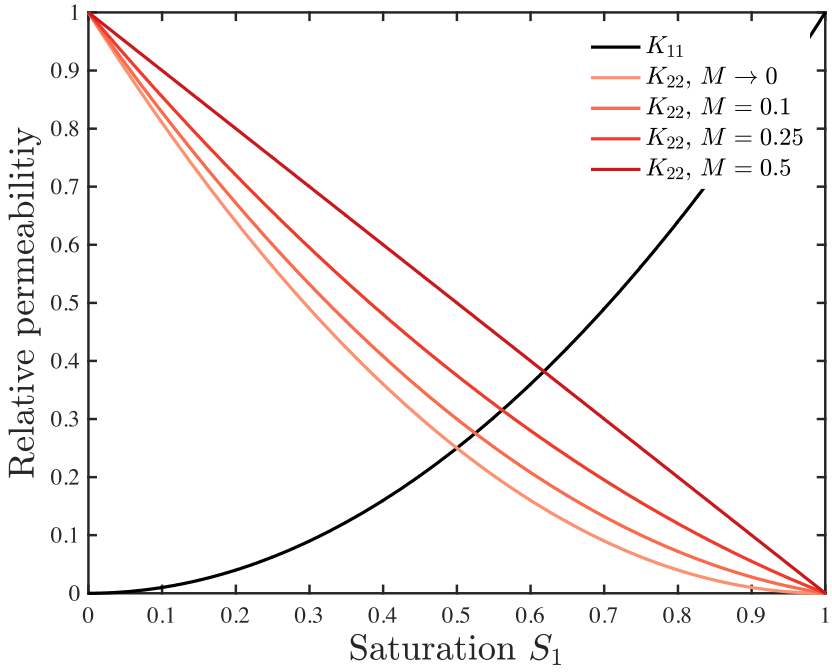

Figure 3: Relative permeability as function of the saturation and the viscosity ratio for the core-annular flow regime.

Concerning the plug flow regime, the relative permeabilities, Eqs. 10, depend only on the unit cell saturation, S_1, the saturation in the plug region, S_{1p} (i.e. the film thickness h) and the viscosity ratio M, as presented in Figs. 4-6. The structure of the relative permeability is consistent with the one obtained for the core-annular flow regimes: in fact, the relative permeability curve of the non-wetting phase (K_{22}) for the core-annular flow regime represents a lower bound for the relative permeability in the plug flow regime at a fixed saturation and when $M < \sim 0.4$. On the other hand, the flux of wetting phase is higher for the plug flow regimes, as expected. In addition, $K_{11} \to 1$ when both $S_1 \to 1$ and $S_{1p} \to 1$.

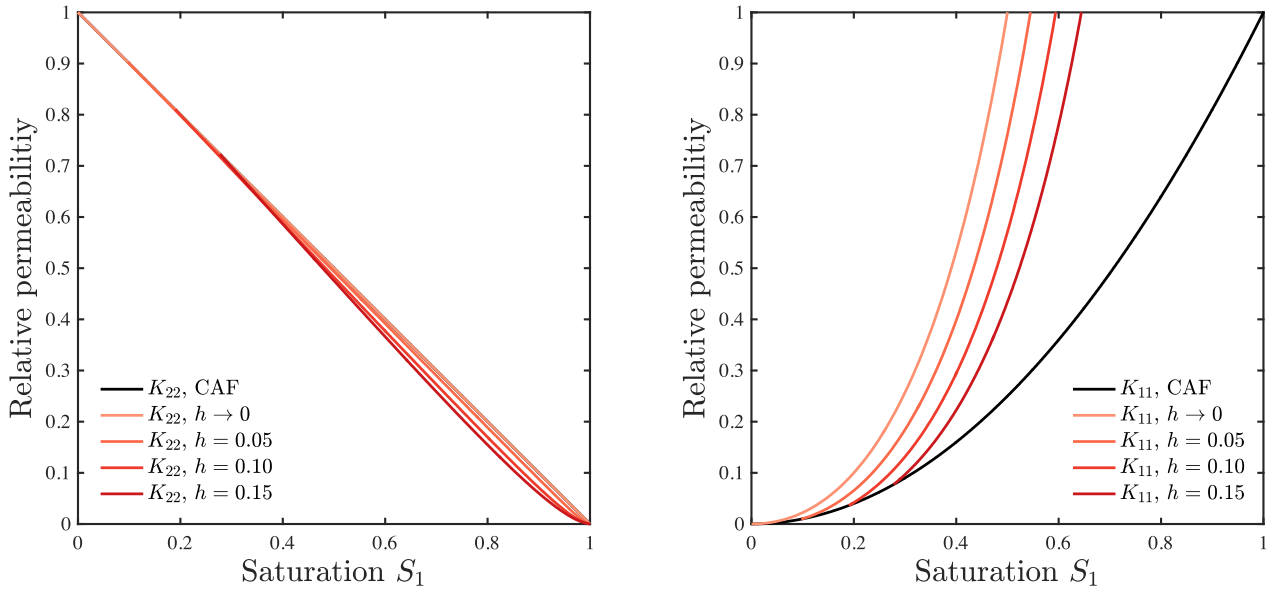

Figure 4: Relative permeabilities K_{22} (left) and K_{11} (right) in terms of the saturation and the film thickness of the plug flow regime M=0.5

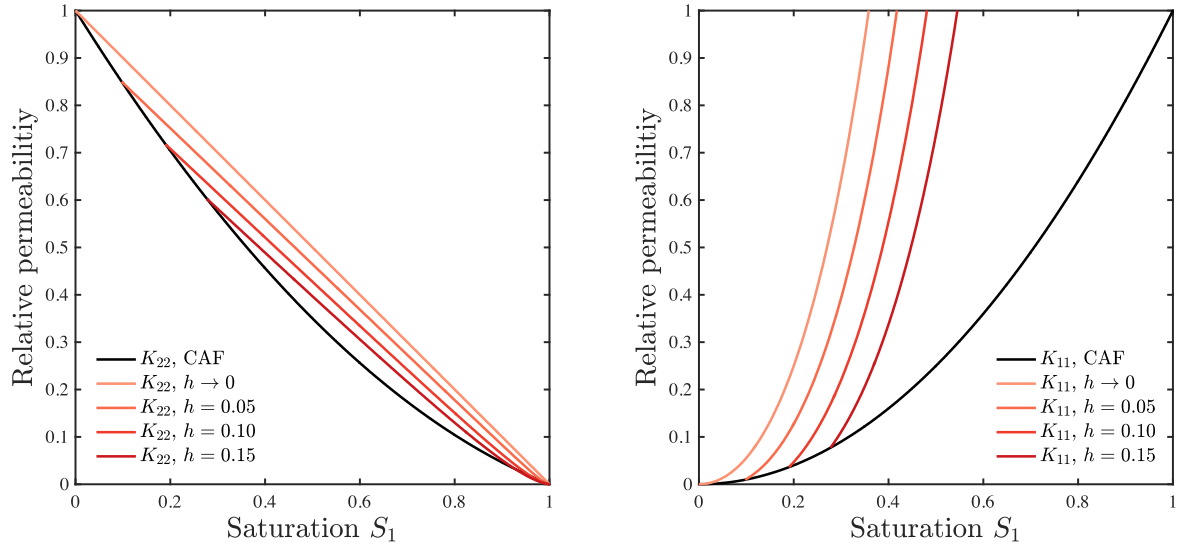

Figure 5: Relative permeabilities as function of the saturation and the film thickness of the plug flow regime M=0.2

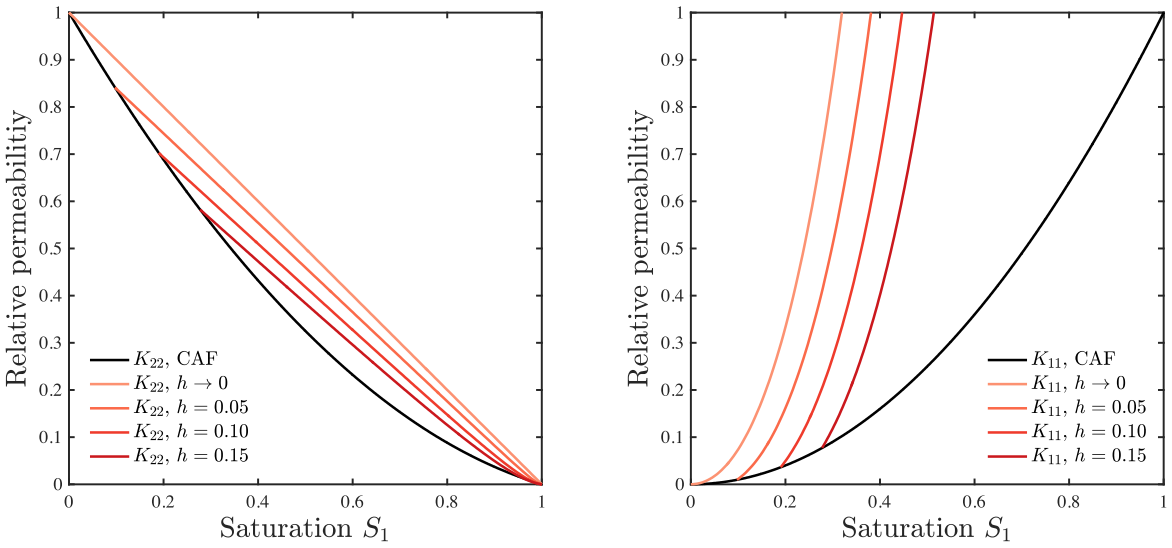

Figure 6: Relative permeabilities as function of the saturation and the film thickness of the plug flow regime M=0.15

In Figs. 4-6 the film thickness of the wetting phase is assumed to be known and it represents the only input parameter of the model. We want to emphasize that estimation for the film thickness is physical-based and it is not a fitting parameter. It can be estimated from XCT microtomographic experiments or analytical models. In the geothermal context, the correlation by *Bretherton* (1961), which has been developed for the case of a non-viscous bubble, can provides a first order estimate of h once the capillary number is estimated according to,

$$h = 1.34\, Ca^{\frac{2}{3}}. \tag{9}$$

Note that in the limit of thin film (surrounding the bubble), $h \to 0$, one obtains $K_{22} = (1 - S_1)$. For viscosity ratio close to $M = 0.5$ the relative permeability of the non-wetting phase converges to the same limit independently from the film thickness, see Fig. 4, while, for lower viscosity ratios, increasing the film thickness yields to a lower relative permeability, see Figs. 5-6.

In order to quantify the effect of the flow regime on the relative permeability curves, we compute the relative error between the relative permeability for the core-annular flow regime and the one corresponding to the plug flow regime of the non-wetting phase, defined as

$$e_{K_{22}} = \frac{|K_{22,PLUG} - K_{22,CAF}|}{K_{22,CAF}}, \tag{10}$$

where $K_{22,CAF}$ and $K_{22,PLUG}$ are given in Eq. 4(b) and Eq. 10(b), respectively. The trends of the relative error $e_{K_{22}}$ are presented in Figs. 7-9. When $M = 0.5$, the relative error $e_{K_{22}}$ is almost negligible at low saturation, while it increases and becomes significant for saturation close to unity. Instead, for cases with lower viscosity ratios typical to geothermal systems, differences in the predicted relative permeability is considerable in the whole range of saturation and reaches peaks bigger than 100% with respect the relative permeability computed for core-annular flow, see Figs. 8 and 9. In addition, the case with a very thin film of the wetting phase surrounding the bubble, $h \to 0$, represents always the case where the difference between the core-annular and plug flow relative permeability curves is maximal.

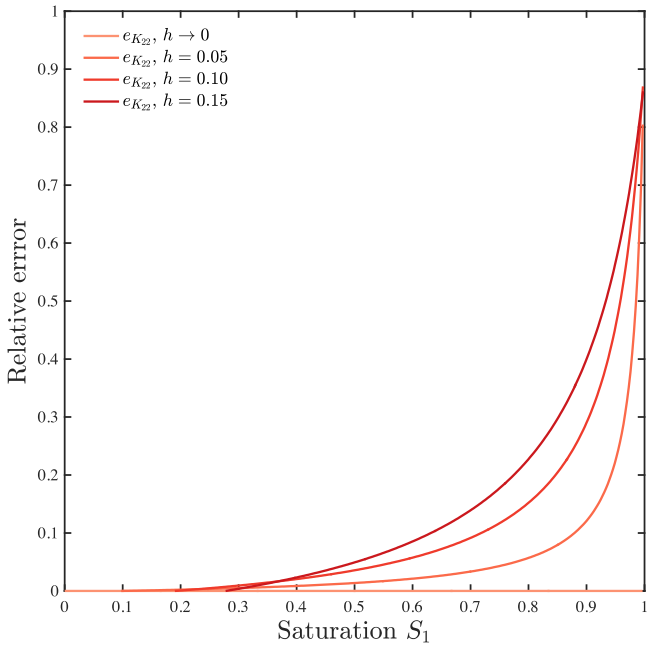

Figure 7: Relative error between the relative permeability of the non-wetting phase assuming core-annular flow and plug flow regime for M=0.5

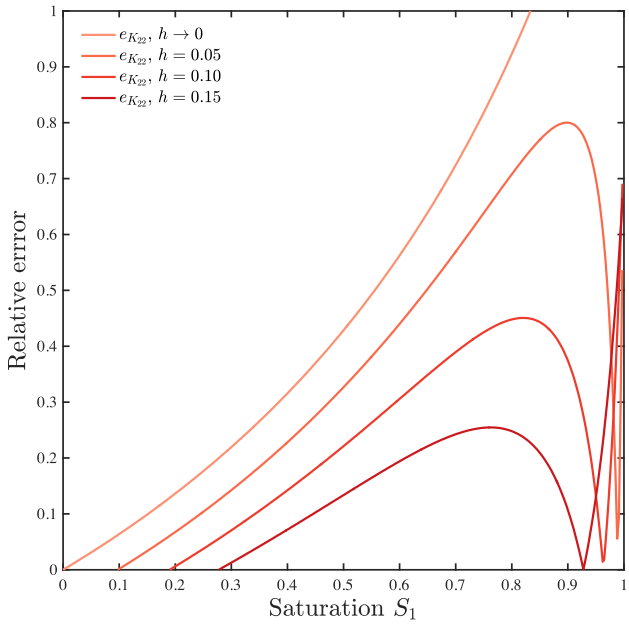

Figure 8: Relative error between the relative permeability of the non-wetting phase assuming core-annular flow and plug flow regime for M=0.2

To sum up, by examination of Figs. 3-9 the influence of the pore-scale flow regime on the relative permeability curves has been investigated: at a fixed saturation, different flow regimes may yield to significant (and not negligible) differences in relative permeability. With our analysis, we have shown that not accounting for the pore-scale flow regimes in the multiphase scenario can lead to severe miss-predictions of filtration velocity in the context of multiphase flows, in general, and geothermal systems, in particular.

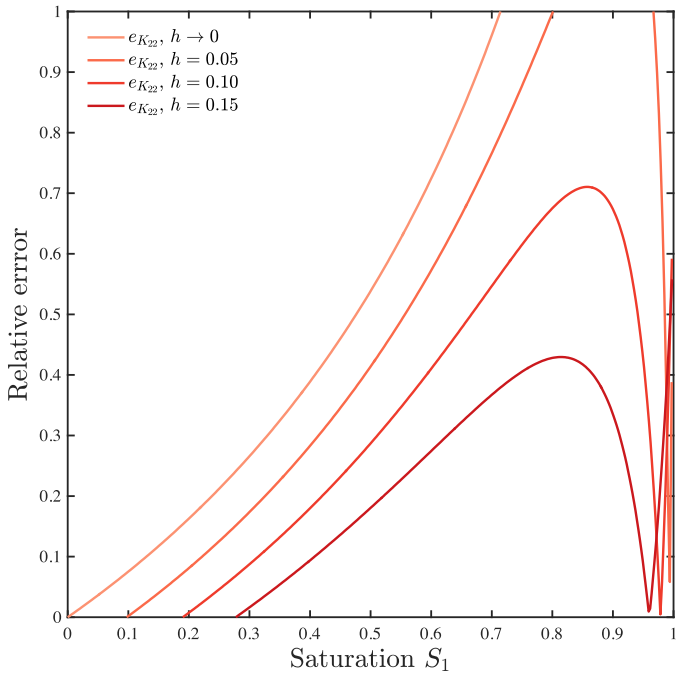

Figure 9: Relative error between the relative permeability of the non-wetting phase assuming core-annular flow and plug flow regime for M=0.15

4. CONCLUSIONS

In this work, we have discussed the upscaled equations based on pore-scale flow-regimes developed by *Picchi and Battiato* (2018) in the context of geothermal engineering applications. In particular, we discussed the trends of the relative permeability curves of the wetting and the non-wetting phase for two basic flow regimes at the pore scale, i.e. core-annular flow and plug flow regime, referring to range of dimensionless parameters (e.g., the viscosity ratio) typical of geothermal reservoirs. These systems are characterized by small density and viscosity ratios (the liquid phase is much more dense and viscous) and water forms the wetting phase while steam is the non-wetting phase. We showed that the lack of two-phase model predictive capabilities is accentuated when flow regimes are not taken into account: differences in the relative permeability between the core-annular flow and the plug flow regimes at a fixed saturation may be significant. In fact, a satisfactory prediction of the phase filtration velocity in a two-phase system needs to account for the phase topology. Notwithstanding the simplicity of the configuration investigated (flow in a capillary tube), this analysis provides a framework to quantify the importance of topology of the flowing phases on relative permeability estimates. The proposed analytical expressions linking pore-scale topology of the flowing phases and their viscosity ration with relative permeability and saturation, will be generalized to real porous media topologies in future works. Current active research is focusing on the l validation of the proposed closures against numerical experiments and laboratory data published in the literature.

REFERENCES

Armstrong, R. T., J. E. McClure, M. A. Berrill, M. Rücker, S. Schlüter, and S. Berg: Beyond darcy's law: The role of phase topology and ganglion dynamics for two-fluid flow, *Phys. Rev. E*, ***94***, (2016), 043113.

Armstrong, R. T., J. E. McClure, M. A. Berrill, M. Rücker, S. Schlüter, and S. Berg: Flow regimes during immiscible displacement, *Petrophysics*, ***58***, (2017), 10–18.

Auriault, J.-L.: Nonsaturated deformable porous media: Quasistatics, *Transport in Porous Media*, ***2***, (1987), 45–64.

Avraam, D. G., and A. C. Payatakes: Flow regimes and relative permeabilities during steady-state two-phase flow in porous media, *Journal of Fluid Mechanics*, ***293***, (1995), 207–236.

Bear, J.: *Dynamics of Fluids in Porous Media*, Dover Civil and Mechanical Engineering Series, Dover, (1972).

Brauner, N.: On the relations between two-phase flows under reduced gravity and earth experiment, *International Communications in Heat and Mass Transfer*, ***17***, (1990), 271 – 281.

Bretherton, F. P.: The motion of long bubbles in tubes, *Journal of Fluid Mechanics*, ***10***, (1961), 166–188.

Daly, K. R., and T. Roose: Homogenization of two fluid flow in porous media, *Proceedings of the Royal Society of London A: Mathematical, Physical and Engineering Sciences*, **471**, (2015), 2176.

Datta, S. S., J.-B. Dupin, and D. A. Weitz: Fluid breakup during simultaneous two-phase flow through a three-dimensional porous medium, *Physics of Fluids*, ***26***, (2014), 062004.

Gao, Y., Q. Lin, B. Bijeljic, and M. J. Blunt: X-ray microtomography of intermittency in multiphase flow at steady state using a differential imaging method, *Water Resources Research*, ***53***, (2017), 10,274–10,292.

Gray, W. G., A. L. Dye, J. E. McClure, L. J. Pyrak-Nolte, and C. T. Miller: On the dynamics and kinematics of two-fluid-phase flow in porous media, *Water Resources Research*, ***51***, (2015),5365–5381.

Hassanizadeh, M., and W. G. Gray: General conservation equations for multi-phase systems: 3. constitutive theory for porous media flow, *Advances in Water Resources*, ***3***, (1980), 25 – 40.

Hassanizadeh, S., and W. G. Gray: Mechanics and thermodynamics of multiphase flow in porous media including interphase boundaries, *Advances in Water Resources*, ***13***, (1990), 169 – 186.

Horne, R.N.: 6 - Characterization, evaluation, and interpretation of well data, In Geothermal Power Generation, *Woodhead Publishing*, (2016), 141-163.

Hornung, U.: *Homogenization and Porous Media*, Springer-Verlag New York, Inc., New York, NY, USA, (1997).

Lasseux, D., A. Ahmadi, and A. A. A. Arani: Two-phase inertial flow in homo- geneous porous media: A theoretical derivation of a macroscopic model, *Transport in Porous Media*, ***75***, (2008), 371–400.

Ling, B., Bao, J., Oostrom, M., Ilenia Battiato, Tartakovsky, A.M., Modeling variability in porescale multiphase flow experiments, Advances in Water Resources, **105**, (2017), 29-38.

McClure, J. E., M. A. Berrill, W. G. Gray, and C. T. Miller: Influence of phase connectivity on the relationship among capillary pressure, fluid saturation, and inter- facial area in two-fluid-phase porous medium systems, *Phys. Rev. E*, ***94***, (2016), 033102.

Miller, C. T., and W. G. Gray: Thermodynamically constrained averaging theory approach for modeling flow and transport phenomena in porous medium systems: 2. foundation, *Advances in Water Resources*, ***28***, (2005), 181 – 202.

Niessner, J., and S. M. Hassanizadeh (2008), A model for two-phase flow in porous media including fluid-fluid interfacial area, *Water Resources Research*, ***44***, (2009), w08439.

Picchi, D., Ullmann, A., and Brauner, N.: Modelling of core-annular and plug flows of Newtonian/non-Newtonian shear-thinning fluids in pipes and capillary tubes, *International Journal Multiphase Flow*, (2018) *paper in press*.

Picchi, D., Battiato, I.: Upscaling of immiscible two-phase flow in porous media: flow regimes and applicability conditions, *Water Resources Research, in preparation.*

Reynolds, C. A., H. Menke, M. Andrew, M. J. Blunt, and S. Krevor: Dynamic fluid connectivity during steady-state multiphase flow in a sandstone, *Proceedings of the National Academy of Sciences*, ***114***, (2017), 8187–8192.

Rucker, M., S. Berg, R. T. Armstrong, A. Georgiadis, H. Ott, A. Schwing, R. Neiteler, N. Brussee, A. Makurat, L. Leu, M. Wolf, F. Khan, F. Enzmann, and M. Kersten: From connected pathway flow to ganglion dynamics, *Geophysical Research Letters*, ***42***, (2015), 3888–3894.

Whitaker, S.: Flow in porous media ii: The governing equations for immiscible, two- phase flow, *Transport in Porous Media*, *1*, (1986), 105–125.

Xu, X., and X. Wang: Non-Darcy behavior of two-phase channel flow, *Phys. Rev. E*, ***90***, (2014), 023010.